CHARACTERISTICS OF THE POLAR ASSEMBLY AND DISASSEMBLY OF MICROTUBULES OBSERVED IN VITRO BY DARKFIELD LIGHT MICROSCOPY

KEITH SUMMERS and MARC W. KIRSCHNER

From the Department of Biochemistry and Biophysics, University of California, San Francisco, California 94143

ABSTRACT

We describe here the continuous observations of the polymerization of individual microtubules in vitro by darkfield microscopy. In homogeneous preparations we verify that polymerization can occur onto both ends of microtubules. The assembly of microtubules is polar, with one end growing at three times the rate of the other. The differential rate of elongation can be used to determine the polarity of growth off cellular nucleating centers. We show that the microtubules grow off the proximal end of ciliary axonemes at a growth rate equal to that of the slow growing end of free microtubules, while growth off the distal end proceeds at the same rate as the fast growing end. Applying this technique to microtubule growth from metaphase chromosomes isolated from HeLa and CHO cells, we demonstrate that chromosomes initiate polymerization with the fast growing end facing away from the chromosome nucleation site. The opposite ends of free microtubules show different sensitivities to microtubule depolymerizing agents such as low temperature, Ca^{++} or colchicine as measured directly by darkfield microscopy. The differing rates of assembly and disassembly of each end of a microtubule suggest that a difference in polarity of growth off nucleating sites could serve as one basis for regulating the polymerization of different groups of microtubules in the same cell.

KEY WORDS microtubules · darkfield microscopy · kinetochore · microtubule polarity

During the cell cycle, microtubules are involved in many different functions. Often, several groups of microtubules will be present at one time, each with a unique time of appearance and disappearance in the cell (50, 15). In addition, microtubules of different stability have been described in several structures even within the same cell (5, 36). The mechanism by which the cell controls spatially and temporally the appearance, orientation, stability, and disappearance of groups of microtubules remains, for the most part, unexplained.

One aspect of this problem has been approached by the identification, isolation, and characterization of cell organelles which serve as nucleating centers for microtubule growth (32). Microtubules have been polymerized in vitro from isolated basal bodies, kinetochores in mitotic chromosomes, and pericentriolar material (43, 28, 44, 45, 18, 19, 21). However, in all cases the nature of the polymerization initiating substance is unknown. In some cases, an amorphous cloud of material seems to be

present at the nucleating sites (18, 34, 35).

Another means by which the cell could differentiate among classes of microtubules would be by the production of more than one molecular form of tubulin or the use of different accessory proteins, which are involved in the polymerization of tubulin. The question of tubulin heterogeneity or the role of molecular modifications of tubulin is very complex. Cyclic-AMP-dependent phosphorylation of tubulin and accessory proteins has been demonstrated but the effect of phosphorylation on the system remains unknown (10, 17, 37, 40). Similarly, enzymes capable of adding and removing a tyrosine residue specifically on the carboxyl terminal of the α subunit of tubulin are known but no effect of this unusual modification on polymerization has been detected (4, 33). Evidence to explain how accessory proteins might control microtubule polymerization in vivo is also generally lacking, though there has been a correlation made between their presence in the brain tissue of developing rats and the general polymerizability of the tubulin extracted from this tissue (39, 14).

Another potential basis for spatial and temporal differentiation among groups of microtubules within a cell comes from the polar nature of microtubules themselves. Microtubules are intrinsically polar as indicated by the subunit lattice structure seen by X-ray diffraction and electron microscopy (20, 3, 12, 9). The intrinsic polarity is also indicated by the fact that tubulin polymerizes to a different extent off the proximal and distal ends of flagellar microtubules (2, 6, 31, 24, 25, 54). If cells were able to initiate microtubule polymerization from nucleation centers with a specific polarity and if they also possessed a mechanism for differentiating between such polar microtubules, they would have an effective control system for discrimination between two groups of microtubules.

To investigate the role of polarity in microtubule polymerization and depolymerization under a variety of conditions, we have observed the growth of individual microtubules by darkfield light microscopy. This technique has been used previously to study ATP-induced sliding of doublet microtubules of flagellar axonemes (46) and the movement of bacterial flagella (26). Observations on reconstituted neural microtubules have also been reported (25, 54, 47). By using darkfield light microscopy it is possible, in principle, to make continuous observations on individual microtubules while at the same time varying their environment. It is then possible to observe changes occurring at either end of single microtubules. Experiments can therefore be performed with homogeneous preparations of microtubules, whereas in electron microscope experiments the nucleating structure must be physically different from the polymerizing microtubule so that the point of nucleation can be identified (2, 6, 31, 24, 25, 54). These experiments also avoid the potentially damaging procedures of fixation, staining, and drying required for electron microscopy. The ability to study the dynamics of the assembly of individual microtubules has enabled us to develop methods for assessing their polarity. We have applied these methods here to determine the polarity of microtubule growth off cellular nucleating sites. Polarity, in these cases, can be determined if it is assumed that subunits can only add at the free end. The results obtained here complement those recently obtained where polarity is assessed by looking at the change in bulk microtubule length. In the case of polarity of kinetochore growth, our experiments support the recent analysis by Borisy (7) using extent of assembly, as judged by electron microscopy, to analyze the rate of microtubule polymerization.

MATERIALS AND METHODS

Microtubule protein was prepared from hog brain tissue as described previously (51). The protein was stored at −20°C in 8 M glycerol. Before each experiment, a sample was diluted into an equal volume of polymerization buffer (0.1 M MES (2-[*N*-morpholino]ethane sulfonic acid), pH 6.4, 2 mM EGTA, 1 mM mercaptoethanol, 0.5 mM $MgCl_2$, 0.1 mM EDTA, 1 mM GTP), polymerized at 37°C, and the microtubules were collected by centrifuging at 75,000 *g* for 30 min. The pellet of microtubules was then resuspended in polymerization buffer and put on ice. After allowing 20 min for depolymerization, the sample was centrifuged again at 75,000 *g* for 30 min to remove insoluble aggregates.

Chromosomes were isolated from mitotic CHO cells by an adaptation of the methods of Gould and Borisy (18). CHO cells were grown to near confluence in 100-mm culture flasks in F-10 medium. Mitotic cells were shaken loose from their culture bottle and collected by centrifuging at 500 *g* for 5 min. The pellet of cells was gently rinsed with distilled water and then suspended in 0.1 ml of distilled water. After 1 min, 0.1 ml of 0.1 M Mes pH 6.4, 0.5 mM $MgCl_2$, 0.5% Triton X-100 was added and the cells were lysed by forcing the suspension through a blunt syringe needle held against the bottom of the tube. In most cases, 0.4 ml of microtubule protein

was added immediately and the sample was incubated at 37°C for 5 min. These chromosome preparations were used immediately for experiments since the chromosome morphology tended to deteriorate after a few hours at room temperature. In a few experiments, chromosomes were preserved by adding 0.5 mM $CaCl_2$ and 1 M hexylene glycol to the lysing media. Such chromosomes were stable at 0°C for several hours. In addition, we obtained chromosomes from colchicine-arrested HeLa cells from U. K. Laemmli (Princeton University) (1).

Axonemes were prepared from cilia detached from *Tetrahymena* by exposing a concentrated suspension of the cells to 1 mM dibucaine. The membranes were removed by suspending the cilia in 0.1% Triton, 0.1 M Mes, pH 6.4, 0.5 mM $MgCl_2$.

Observations were made with a Zeiss Axiomat light microscope (Carl Zeiss, Inc., N. Y.) with a 200-watt mercury arc light source fitted with infrared filters and a darkfield condenser. In some cases, an image intensifier (obtained from the U. S. Army) was employed between the photographic screen and the 35-mm camera. Photographs were taken on a Kodak Tri-X film at an ASA setting of 1600 on the automatic camera of the microscope. This film was developed in Kodak HC-110 dilution B for 1.5 times the recommended time. Under these conditions, exposure times ranged around 1 s. Some pictures were taken on Kodak SO-410 film developed in HC-110 dilution D for the recommended time. With this film, exposure times were ~4 s.

Microscope slides were specially prepared to allow precise control of flow in the region of observation. Grooves were cut on either end of the region to be covered by the coverglass. One groove was used as a well to hold the various solutions. The other groove was covered with a sheet of flat rubber pierced obliquely by a syringe needle. The needle was connected by tubing to a Gibson microliter pipetting device. By using silicone grease to form the walls of a channel between the grooves and to seal the syringe needle into place, a closed system was formed. Microscope slides and coverslips were scrupulously cleaned for each experiment.

Analysis of large volumes of data was facilitated by computer processing. Spatial coordinates of microtubules were transferred from film into an IBM 370 by projecting each frame into a Tektronix digitizer and manually identifying the ends of each microtubule with the electronic marking pen. Subsequent calculations yielded graphs of incremental growth of each end of each microtubule. Growth rates were calculated from these graphs by the method of least squares.

Protein concentrations were calculated by the method of Lowry et al. (27).

RESULTS

Polymerization of Microtubule Protein

The initial steps of the assembly of microtubules from monomers and oligomers of tubulin are difficult to visualize by darkfield microscopy. The polymeric components in the initial steps scatter light less intensely than do microtubules. Since they also move rapidly around by Brownian motion, it has not been possible to photograph the nucleation process in real time. These components have been photographed by darkfield microscopy and electron microscopy after fixation with glutaraldehyde (25, 47) and suggest that the flexible intermediates could represent protofilament sheets, which have been reported to be present during the assembly reaction both in vitro and in vivo (23, 11, 8, 41, 49).

It is possible, however, to photograph clearly the elongation of microtubules, which takes place in the later phase of polymerization. Microtubules usually adhere to the glass slide at some point and are thus restricted in their random motion. They scatter sufficient light to be detectable with a 1-s exposure or shorter exposure with an image intensifier. In a typical experiment, a sample of microtubule protein is polymerized at 37°C under standard conditions, diluted with purification buffer, and introduced into the slide chamber. Some microtubules settle onto the surface of the slide and become attached. Depolymerized microtubule protein is then placed in the sample well of the slide where it was prewarmed to room temperature and then rapidly flowed into the area of observation. The flow of prewarmed unpolymerized subunits past microtubule fragments serves two purposes. First, the concentration of protein is held constant and, therefore, not diminished by polymerization. Second, and most important for the darkfield method, the unpolymerized solution appears transparent due to its low capacity to scatter light. Photographs are taken at intervals of 10–20 s. From the photographs of a typical experiment, the elongation of ~20 of the most clearly distinguishable microtubules can be followed for 5–15 frames. In all, experiments on the growth of isolated microtubules involved the analysis of ~400 microtubules in over 600 frames.

Fig. 1 shows portions of two sequences each containing about five growing microtubules. The position of the microtubule ends can be measured relative to brightly scattering dust spots on the glass surface. It is clear from the sequences that each microtubule grows from both ends but that growth occurs faster off one of the ends. For the analysis, the position of each end of each micro-

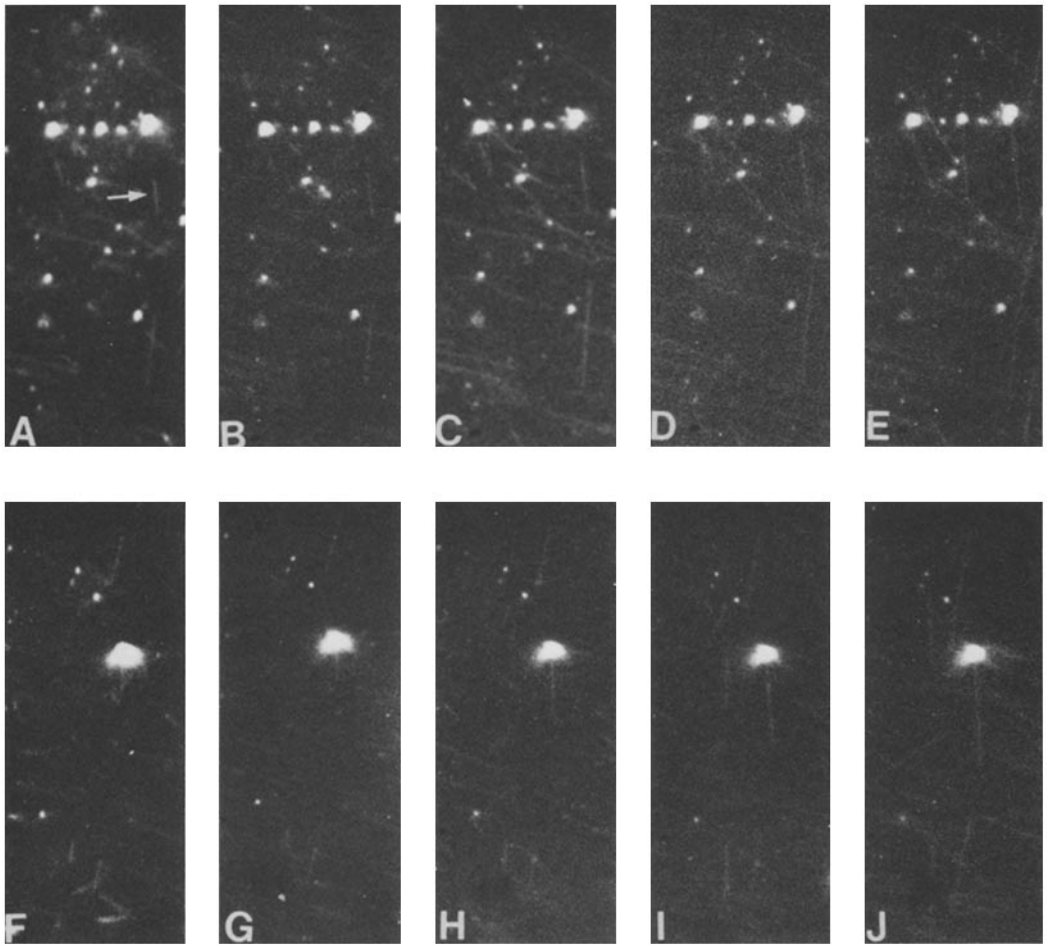

FIGURE 1 Elongation of individual microtubules by darkfield microscopy. Two sequences (*A–E* and *F–J*) representing portions of a field are shown to demonstrate microtubule elongation. A number of growing microtubules are visible (one of which is denoted by arrows). The bright spots are dust particles with which one can align the photographs. The concentration of microtubule protein was 1.3 mg/ml and temperature was 24°C. × 1,390.

tubule is determined relative to a coordinate system defined by the invariant position of dust spots. Growth rate can then be calculated (with the help of a computer) by comparing frames. Fig. 2 is an example of a graph of the growth of each end of a single microtubule. The starting points of these experiments were microtubule segments 3–7 μm in length. The average scatter in the data for each point is ~0.5 μm, which represents errors primarily in superposition of frames and in accurately determining the position of the end of a microtubule. The rate of growth calculated from Fig. 2 is 1.1 μm/min for the fast growing end and 0.28 μm/min for the slow growing end. Under the condition of this experiment, therefore, the fast and slow growing ends differ about threefold in their rates of growth.

Data from graphs generated by the computer were averaged for all microtubules within an experiment, excluding those cases where growth was not observed on both ends of the microtubule. This occurred in about one-third of all microtubules measured. Absence of growth was noted equally as often on the fast as on the slow growing end. The other end continued to grow at either the typical slow or fast rate. It was assumed that lack of growh on one end was due to the microtubule's being attached to the microscope slide in such a

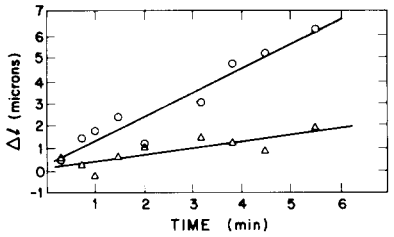

FIGURE 2 Growth of each end of a single microtubule. The increase in length $\Delta\ell$ in microns is plotted versus time in minutes. The incremental distances of the fast growing ends are denoted by 0 and the slow growing end by Δ. This plot is taken directly from the computer analyzed data and the straight line is a least squares fit. The rate of growth of the fast end is 1.1 μm/min, the slow end 0.28 μm/min. Microtubule protein concentration was 1.4 mg/ml and the temperature 24°C.

manner as to block that end for assembly.

The growth rates for the fast and slow growing ends in a single sequence fell into two classes as shown in Fig. 3. There was some variation in the rates of growth, part of which may be due to errors in measurement, part of which may be due to differences in the protein from one experiment to another, and part of which may be due to inherent fluctuations in growth rates of individual microtubules within a given experiment. The rate of growth of the fast end averaged over all experiments in Fig. 3 was 1.0 μm/min and of the slow end was 0.40 μm/min. These, of course, refer to the exact buffer conditions at 24°C.

The fast and slow ends differed also in the concentration dependence of their rates of growth, as shown in Fig. 4. Although at concentrations above 0.5 mg/ml the rate of growth of either end is proportional to concentration suggesting a first-order process, these rates do not extrapolate to zero at zero protein concentration. This may suggest a limitation of this method to give absolute rate data. Low concentrations could not be easily studied experimentally due to the slow rate of growth at 25°C. It is also possible that the concentration dependence could be different than the first order below 0.5 mg/ml at 25°C or that we may be observing some effect of treadmilling observed by Margolis and Wilson (29). The apparent first-order polymerization rates for the fast and slow growing ends are 0.31 and 0.10 μm/min 1/g, respectively. Assuming that the tubulin molecule has a molecular weight of 10^5 (53), we can calculate the rate of addition of a mole of subunits per mole of microtubule ends. This is a second-order rate

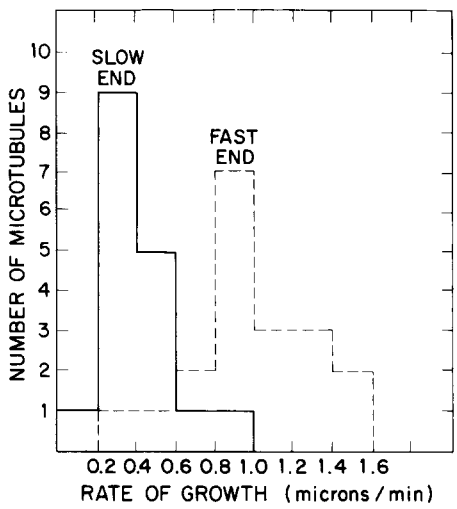

FIGURE 3 Distribution of rates of growth of the fast and slow growing ends in a single sequence. The experimental conditions were the same as in Fig. 2.

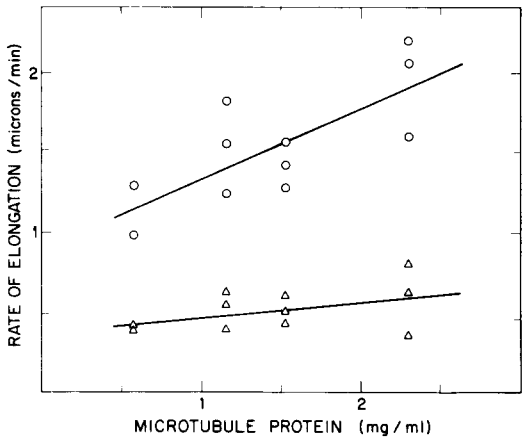

FIGURE 4 Effect of protein concentration on the rate of elongation of the fast and slow growing ends. Each point represents a separate experiment consisting of measurements of ~20 microtubules. The upper line (0) represents the fast growing end, the lower (Δ) the slow growing end.

constant and its value is 9.3×10^5 s^{-1} M^{-1} for the fast and 3.0×10^5 s^{-1} M^{-1} for the slow growing ends. Accurate kinetic data for microtubule assembly using turbidity as an assay were obtained by Johnson and Borisy (22) who calculated an overall rate constant of 1.9×10^6 s^{-1} M^{-1} under similar buffer conditions, except that their data were obtained at 30°C whereas ours were measured at

25°C. To compare these two measurements, we note that the rate of assembly approximately doubles between 25 at 30°C (16) and that the overall rate of elongation is simply the sum of the rates off each end. Correcting for the temperature and summing the two rates, we calculate a value for the overall rate of elongation of $2.5 \times 10^6\ M^{-1}\ s^{-1}$ at 30°C as compared to the value of Johnson and Borisy of $1.9 \times 10^6\ M^{-1}\ s^{-1}$. There is therefore very close agreement between these different methods of measurement.

One casual observation made in the course of these experiments is that if duplicate samples are polymerized, one by rapidly warming to 37°C and the other by slowly warming to 37°C, the latter sample will have microtubules which are much longer than those in the former. Hysteresis and overshoot in assembly of tobacco mosaic virus assembly into rods has been noted by Scheele et al. (38). In that case, rapid warming produced long rods while in this case rapid warming produces shorter microtubules. In the case of microtubule assembly, it would seem that the nucleation rate increases faster with temperature than the elongation rate.

Growth off Ciliary Axonemes

The extent of assembly of brain microtubules off flagellar or ciliary axenomes has been demonstrated extensively by electron microscopy (2, 6, 25, 54). The extent of microtubule growth by sampling a population, at one or a few time points, however, may not be an accurate measure of the rate of growth, particularly if the ends differ in their rates of initiation. We, therefore, attempted to measure directly the growth of individual microtubules from the ends of axonemes. We could then compare their growth to that of individual free microtubules in the same field and use this information to determine the relative polarity of free microtubules and axonemal microtubules.

Fig. 5 shows two examples of polymerization nucleated by axonemes isolated from *Tetrahymena* cilia. It is again clear that growth occurs from both ends of the axoneme and that one end grows faster than the other. Table I compares the incremental growth of free microtubules and those nucleated by axonemes in the same field for two separate experiments. Each represents the analysis of over 50 axonemes and free microtubules. The rate of growth of the slow end off axonemes is within experimental error equal to the rate of growth off the slow end of the free microtubules, while the fast ends are also comparable in rate. It is more difficult to distinguish the proximal and distal ends of the axoneme by darkfield microscopy than by electron microscopy. However, these results coupled with those from electron microscope studies indicate that the end with the greatest extent of assembly is also the end with the fastest microtubule growth and corresponds to the distal end of the axoneme. From these experiments we may conclude that the rate of elongation is a useful indication of the polarity of the microtubules. From previous studies (2, 6, 31, 24, 25, 54, 7) we may assume that the proximal end of the axoneme corresponds to the slow end and the distal end, the fast end.

Polarity of Microtubule Growth off Kinetochores of Metaphase Chromosomes

Under the assumption that microtubules can only elongate from their free end, we would postulate that organelles which nucleate microtubule assembly with a specific polarity would be expected to have microtubules whose free ends grow either slowly or fast. Those with free fast growing ends can be termed as having plus polarity and those with free slow growing ends can be termed as having minus polarity, in agreement with the terminology of Borisy (7).

Using the methods described above, we investigated the polarity of microtubule growth off the kinetochores of metaphase chromosomes. These experiments were based on earlier work which showed that it was possible to polymerize microtubules off metaphase chromosomes in vitro (28, 44, 48). An extract of mitotic CHO cells was made by a modification of the methods of Gould and Borisy (reference 18, see Materials and Methods). Alternatively, metaphase chromosomes were obtained from the HeLa cells by the method of Adolph, Cheng, and Laemmli (1). Both sources of chromosomes behaved identically. In some experiments, chromosomes were allowed first to become attached to the microscope slide and then were rinsed with purification buffer. Depolymerized microtubule protein was then flowed in and the microtubules were allowed to polymerize. In other experiments, however, the microtubule protein was added to the chromosomes (immediately after cell lysis) and incubated at 37°C for 5 min. The advantage of the latter technique was that a higher fraction of the chromosomes had microtubules

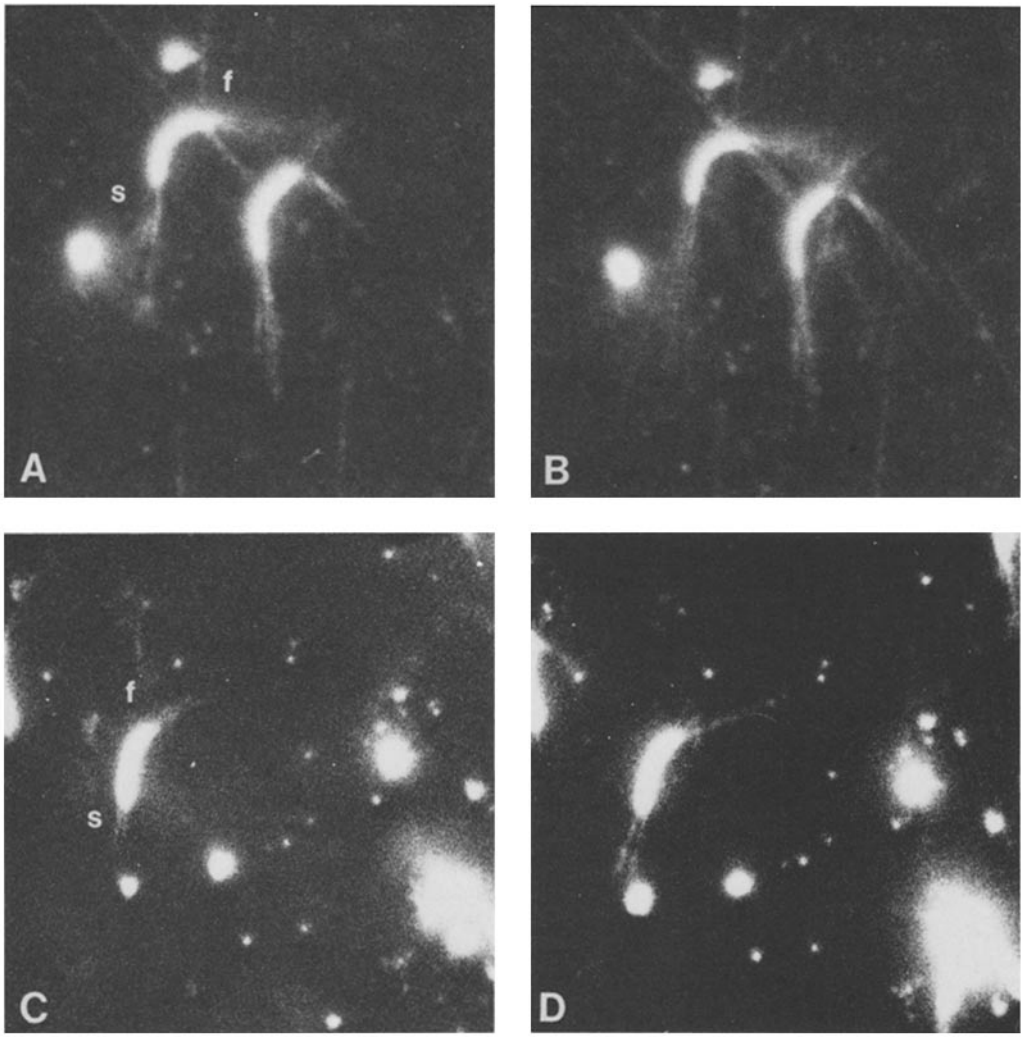

FIGURE 5 Polymerization of microtubules from ciliary axonemes. *A* and *B*, and *C* and *D* are two pairs of photographs showing growth of microtubules off ciliary axonemes. The time interval in both cases was ~4 min, and the protein concentration was ~1 mg/ml. The fast growing end is denoted by *f* and the slow by *s*. × 2,380.

inserting into them. The latter method also served to verify that the microtubules were actually attached to a specific point in the chromosome since the microtubules remained in place throughout the process of dilution, settling, and rinsing of the chromosomes. In all cases, they seemed to radiate from a small region of the chromosome. This could be most easily observed when the chromosome moved or when it was disturbed by convection in the solution. Kinetochore microtubules were characteristically few in number (32, 28, 44, 19, 34, 35) pointed inward toward a single point in the body of the chromosomes (see Fig. 6). They often inserted into the chromosome above the plane of the glass slide. Identification of such microtubules was easier than might be implied from the photographs since, unlike the microtubules on a glass surface, the microtubules inserting into the kinetochore were not all in the same plane and could only be properly visualized by varying the focus of the microscope. In addition, since they were anchored only at one end they showed more movement due

TABLE I

Comparison of Axonome Nucleated and Free Microtubule Growth

	Free microtubules		Axoneme nucleated	
	Fast end	Slow end	Fast end	Slow end
Exp. 1	4.2 ± 2.1	1.3 ± 0.3	5.1 ± 2.3	1.4 ± 0.4
Exp. 2	2.3 ± 1.1	0.8 ± 0.4	2.3 ± 0.9	0.8± 0.4

Microtubule growth was measured by comparing the lengths of individual microtubules at an interval of ~5 min at 25°C. The left hand column shows the average incremental change in the length of both ends of individual free microtubules, and the right hand column shows the average incremental change in the length of both ends of individual axoneme nucleated microtubules. Both the lengths and standard deviations are given in microns. 50–100 microtubules were analyzed in each experiment.

to convective disturbances and Brownian motion so that some always appeared blurred due to the relatively slow photographic exposure.

It is impossible to tell by darkfield microscopy whether all the microtubules arise from the kinetochore. As the chromosomes were washed, agitated, and settled, the microtubules gave the appearance of growing from one region. Similar regrowth experiments analyzed by electron microscope (28, 44, 48), and particularly experiments by Gould and Borisy (19), showed that microtubules appear to regrow from the kinetochore. We cannot rule out some adventitious growth, but if that occurred it would be of the uniform polarity (see below).

In darkfield microscopy chromosomes appear as bright spots of light, distinguishable from dust spots only by the organized microtubule growth. Chromosomes swell and lose their characteristic shape when placed in media lacking calcium or hexylene glycol, and we were concerned that we could not identify them definitively. Therefore, subsequent to each polymerization experiment, ethidium bromide was flushed through the field and the preparation was examined by fluorescence illumination. Only chromosomes fluorescenced intensely with ethidium bromide and this method conclusively distinguished chromosomes from debris which scattered comparable amounts of light (see Fig. 6*d*).

As shown in Fig. 6 microtubule growth from chromosomes can be easily observed. We examined the rate of growth of ~150 microtubules growing from 30 chromosomes in three separate experiments involving both HeLa and CHO cells. The usual interval of study was ~5 min. As shown in Table II the free microtubules showed a threefold difference in rates of elongation, in agreement with the data given in Figs. 1, 2, and 3. A comparison of the incremental growth of chromosome-nucleated and free microtubules in Table II shows clearly that chromosomal microtubules grow at a rate equal to that of the fast growing ends of the free microtubules. Among 150 chromosomal microtubules, only six appeared to grow at a rate less than half that of the fast growing end. By this criterion, microtubules grow from kinetochores of metaphase chromosomes with plus polarity.

Polarity of Microtubule Disassembly

Various depolymerizing agents were studied to see whether they too had a polar effect on microtubule assembly. Low temperature (4°C) and Ca^{++} (1 mM) cause disassembly of microtubules with a threefold bias of one end over the other. Fig. 7 illustrates this for low-temperature-induced disassembly. More selective than either of these agents is colchicine. Under in vitro conditions 25°C disassembly by 0.25 mM colchicine proceeds very slowly, taking ~1 h. However, disassembly proceeds from only one end. Experiments with flagellar axonemes indicate that the effect is on the distal or fast growing end. This has been confirmed by electron microscopy (Witman, Weingarten, and Kirschner, unpublished results).

DISCUSSION

Despite the fact that their thickness is far below the resolution of the light microscope, microtubules are readily observable by darkfield light microscopy. The apparent thickness of the microtubules is ~0.3 μm in most of our exposures. Bacterial flagella, while they are even smaller than microtubules, have been visualized previously by darkfield microscopy where the limiting factor is only the amount of light they scatter (26). To visualize the growth of microtubules, it was necessary to overcome some technical limitations imposed by the sensitivity of the film, Brownian motion, and background light scattering at high protein concentrations. These limitations put certain constraints on the experimental design. In interpreting these experiments, it has been assumed that the effects of the glass surface are limited to the occasional complete blockage of polymerization on one end of a microtubule, as

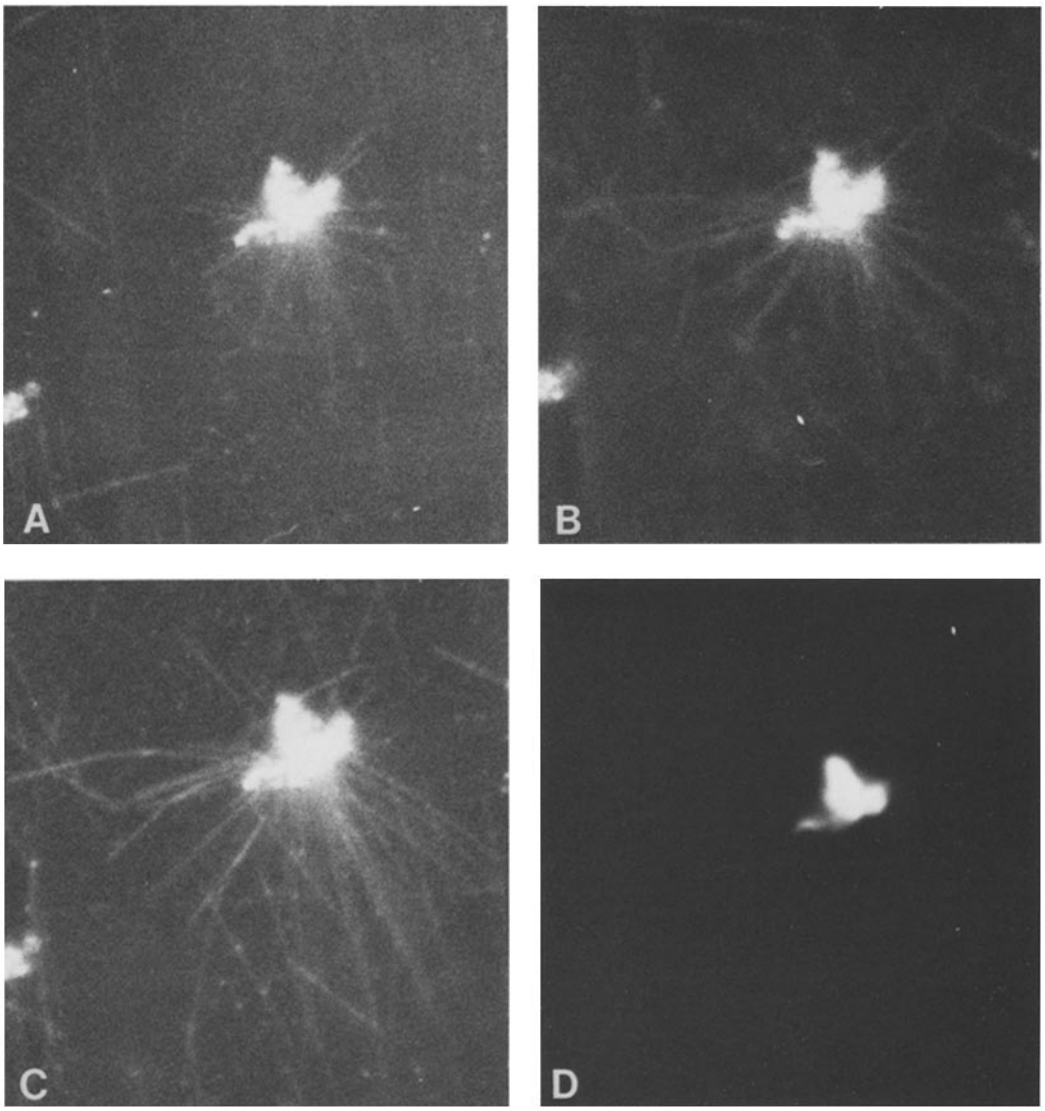

FIGURE 6 Polymerization of microtubules off metaphase CHO chromosomes. (*A*–C) Sequence of microtubule growth off metaphase chromosome. (*D*) Ethidium bromide stained, fluorescence micrograph of same field. × 1,870.

discussed above. In the initial phases of an experiment, microtubules seem attached to the microscope slide at only one point along their length (usually near one end). Some pivoting around this point can occur during the flow of the surrounding solution, and the effect of this rotation on length determination was accounted for in the computer program. During the course of an experiment, microtubules apparently become attached at more than one point and rotation of the microtubules in the flow decreases. Yet, no dramatic changes in the characteristics of polymerization were noted. Nevertheless, we must consider the fact that some of the scatter in the measured rates of polymerization may have been due to some effect of the proximity of the glass surface to the ends of the microtubule.

To minimize the possibility that the intense light

beam was affecting the polymerization or depolymerization of microtubules, parallel experiments were conducted with either a 410 barrier filter, which eliminated all ultraviolet radiation, or a blueglass filter in place. Periodic observations were also made in regions outside the spot of illumination. In only one case was an effect of light noted in the absence of the filter. When attempting to disassemble microtubules with Ca^{++}, we noticed that microtubules within the beam became stabilized against depolymerization while microtubules out of the beam dissolved. Either filter eliminated this effect. The 410 barrier filter was also used with colchicine experiments, since colchicine is photosensitive. In all experiments, the beam of light was diverted away from the specimen between observations.

TABLE II

Comparison of Chromosome Nucleated and Free Microtubule Growth

	Free microtubules		Chromosome nucleated
	Fast end	Slow end	
Exp. 1	6.4 ± 2.2	2.1 ± 1.2	6.5 ± 1.3
Exp. 2	5.5 ± 0.9	2.1 ± 0.9	5.6 ± 1.8
Exp. 3	5.2 ± 0.7	1.6 ± 0.5	5.4 ± 1.4

Microtubule growth was measured by comparing the lengths of individual microtubules at an interval of ~5 min at 25°C. The left hand column shows the average incremental change in the length of both ends of individual free microtubules. The right hand column shows the average incremented change in the length of individual chromosome nucleated microtubules. Both lengths and standard deviations are given in microns. Exps. 1 and 2 refer to CHO chromosome. Exp. 3 refers to HeLa chromosome. ~150 chromosome nucleated and 300 free microtubules were analyzed.

Using darkfield light microscopy we have verified that polymerization can occur onto both ends of microtubules in a homogeneous system. Electron-microscope studies of microtubule polymerization cannot easily distinguish growth on either end. They only qualitatively show that with time microtubules grow longer. In addition, breakage of microtubules and selective adhesion during sample preparation are serious impediments to any quantitative electron microscope analysis. To distinguish growth from each end of a microtubule by electron microscopy, the microtubule must somehow be marked. Olmsted et al. (31) attempted to do this by marking microtubule fragments by diethylaminoethyl (DEAE) dextran and allowing them to elongate. However, Erickson and Voter (13) have shown subsequently that DEAE dextran has a specific effect in promoting tubulin assembly. Nevertheless, the experiments of Olmsted et al. indicated that homogeneous microtubules grow in a biased polar manner, that is, one end grows faster than the other, a result which we have confirmed here.

Continuous observations by darkfield micros-

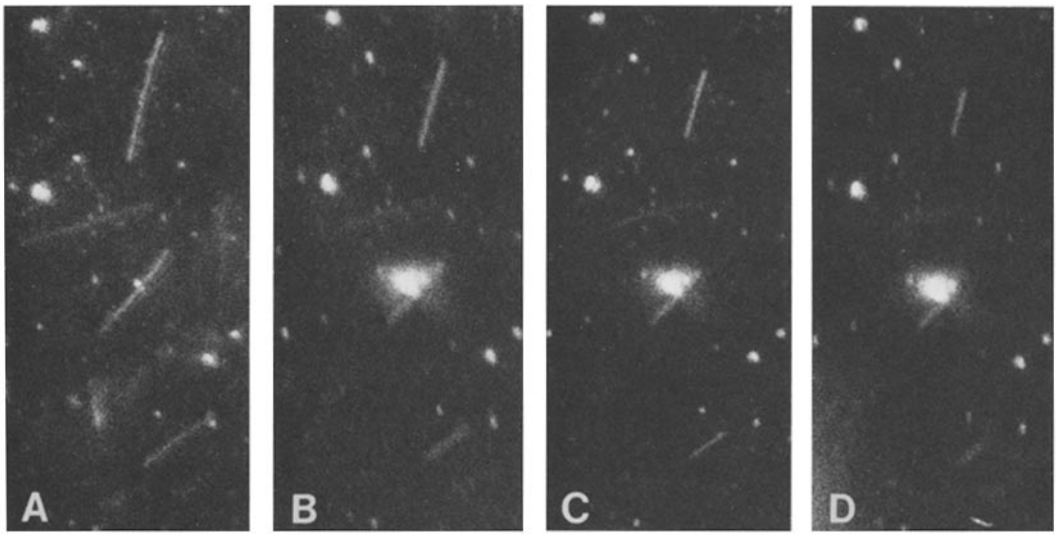

FIGURE 7 Cold depolymerization of free microtubules. Microtubules were polymerized at 37°C, and depolymerized by washing in purification buffer at 4°C. The interval was ~10 s. × 1,870.

copy allow accurate measurements of the rate of growth of each end of individual microtubules without the inaccuracies which occur when populations of microtubules are sampled. In the experiments shown in Figs. 1 and 2, it is clear that microtubule polymerization is polar in nature, proceeding about three times as fast at one end as at the other. The rate of elongation of the fast growing end or plus end increases faster with concentration than that of the slow or minus end (Fig. 4). The data in Fig. 4 can be presented in terms of a pseudo first-order reaction, despite the fact that the rates do not extrapolate to zero at zero protein concentration. However, the sum of the apparent second-order rate constants for elongation from the plus and minus end agree well with the overall elongation rate constantly calculated from the kinetic analysis of their turbidimetric experiments by Johnson, Vallee, and Borisy (22) when a correction is made for the difference in temperature between the two measurements.

In studies reported here, we have explored only a narrow set of experimental conditions. We have used microtubule protein, prepared by cycles of polymerization, which is capable of self assembly under standard buffer conditions and contains proteins in addition to tubulin (13, 52, 30, 42). Other investigations have used preparations depleted in rings and associated proteins which are no longer capable or deficient in self assembly. The current kinetic experiments, extended to other preparations of tubulin and associated proteins, could provide information on the mechanism of microtubule polymerization.

Recently, Margolis and Wilson (29) have reported experiments suggesting that there is an assembly site for tubulin at one end of the microtubule and a disassembly site for tubulin located at the other end. This is an extreme polar model. We find evidence, however, for assembly and for disassembly at each end of individual microtubules. These experiments, however, are not strictly comparable to one another since Margolis and Wilson worked at pseudo-equilibrium conditions, i.e., where the amount of polymerization was a constant, while our experiments were done under steady-state conditions where the amount of polymer increased linearly with time. However, both their experiments and those reported here strongly imply that homogeneous microtubules have a polarity in assembly.

In the studies of nucleated microtubule assembly, we have confirmed the previous observations by electron microscopy (2, 6, 54) and by darkfield microscopy of microtubule populations (25) that microtubules can grow off of both ends of flagellar and ciliary axonemes. The slower growing end of the axoneme has a rate of growth equal to the growth rate off the slow end (minus end) of homogeneous microtubules while the growth rate off the opposite end equals the rate off the fast end (plus end) of free microtubules. Thus, the conclusions concerning polarity based on measurements of the overall extent of polymerization of a population of molecules by electron microscopy are confirmed by continuous observation of the growth of individual microtubules by darkfield microscopy.

The above results have given us confidence in utilizing measurements of the rate of microtubule growth as a measure of the polarity of microtubules. As shown in Fig. 3, there is very little overlap in the distribution of the rates for the fast and slow ends of free microtubules, and similar results are obtained with nucleated assembly from ciliary axonemes. Microtubule growth off metaphase chromosomes as measured by darkfield microscopy (Fig. 6) proceeds at a rate equal to that of the fast growing end (Table II). This suggests strongly that subunits are adding the ends of the microtubules with plus polarity. In particular, the recent experiments of Borisy (7) and coworkers, which determined the polarity of microtubules by measuring the average extent of growth as a function of time, are confirmed by the present experiments. If the growth rate off centrosomes is also plus, then it appears that microtubules in the mitotic spindle are in an antiparallel array (7), as actin in muscle.

The depolymerization experiments with Ca^{++}, low temperature, and colchicine showed that depolymerization again can occur off both ends of microtubules and that it also has a polarity, although no effort was made in these experiments to correlate the polarity of depolymerization with that of polymerization. These experiments can be susceptible to artifact. Earlier experiments with KCl depolymerization were quite misleading since careful analysis later showed that KCl also induced fragmentation of the microtubule as well as inducing depolymerization.

The differential sensitivity of microtubules to depolymerization with various agents and their differential rate of elongation suggest a mechanism

by which a cell could distinguish both spatially and temporally between two groups of microtubules solely on the basis of polarity. By varying the concentration of polymerizable microtubule protein through synthesis or modification of tubulin or associated proteins, the cell could allow assembly to occur only on sites with plus polarity among a set of available nucleating sites of both plus and minus polarity. Once initiated, microtubules growing from plus sites will elongate more rapidly than those on minus sites. Thus, polarity can influence both the appearance and the rate of polymerization of microtubules in the same environment. By adjusting depolymerization conditions to selectively attack either the plus or minus end, the cell could also eliminate or preserve a specific set of microtubules. It is also conceivable that the cell could apply a block to existing microtubules, again being selective, for which end is free. Thus, microtubules of two different stabilities can be created from the same set of subunits based entirely on the polarity of the nucleation centers.

We thank the Department of Biochemical Sciences, Princeton University, where most of this work was performed, for providing the microscopy facilities, U. K. Laemmli, Princeton University, for the gift of HeLa metaphase chromosomes, and Margaret Lopata for preparing *Tetrahymena* axonemes and for aid in the photography.

This work was supported by United States Public Health Service grant GM26875-01, American Cancer Society grant VC213, and, to M. W. Kirschner, support from the Dreyfus Foundation and the Public Health Service Research Career Development Award.

Received for publication 15 March 1979, and in revised form 8 June 1979.

REFERENCES

1. ADOLPH, K. W., S. M. CHENG, and U. K. LAEMMLI. 1977. Role of nonhistone proteins in metaphase chromosome structure. *Cell.* **12**:805–816.
2. ALLEN, C., and G. G. BORISY. 1974. Structural polarity and directional growth of microtubules of *Chlamydomonas* flagella. *J. Mol. Biol.* **90**: 381–402.
3. AMOS, L. A., and A. KLUG. 1974. Arrangement of subunits in flagellar microtubules. *J. Cell Sci.* **14**:523–549.
4. ARCE, C. A., J. A. RODRIGUEZ, H. W. BARRA, and R. CAPUTO. 1975. Incorporation of L-tyrosine, L-phenylalanine and L-3,4-dehydroxyphenylalanine as single units into rat brain tubulin. *Eur. J. Biochem.* **59**:145–149.
5. BEHNKE, O., and A. FORER. 1967. Evidence for four classes of microtubules in individual cells. *J. Cell Sci.* **2**:169–192.
6. BINDER, L. I., DENTLER, W. G. and J. C. ROSENBAUM. 1975. Assembly of chick brain tubulin onto flagellar microtubules from *Chlamydomonas* and sea urchin sperm. *Proc. Natl. Acad. Sci. U. S. A.* **72**:1122–1129.
7. BORISY, G. G. 1978. Polarity of microtubules of the mitotic spindle. *J. Mol. Biol.* **124**:565–570.
8. BRYAN, J. 1976. A quantitative analysis of microtubule elongation. *J. Cell Biol.* **71**:749–767.
9. COHEN, C. S., S. C. HARRISON, and R. G. STEPHENS. 1971. X-ray diffraction of microtubules. *J. Mol. Biol.* **59**:375–380.
10. EIPPER, B. A. 1972. Rat brain microtubule protein: purification and determination of covalently bound phosphate and carbohydrate. *Proc. Natl. Acad. Sci. U. S. A.* **69**:2283–2287.
11. ERICKSON, H. P. 1974. Assembly of microtubules from preformed, ring-shaped protofilaments and 6 S tubulin. *J. Supramol. Struct.* **2**:393–411.
12. ERICKSON, H. P. 1974. Microtubule surface lattice and subunit structure and observations on reassembly. *J. Cell Biol.* **60**:153–167.
13. ERICKSON, H. P., and W. A. VOTER. 1976. Polycation induced assembly of purified tubulin. *Proc. Natl. Acad. Sci. U. S. A.* **73**:2813–2817.
14. FRANCON, J., A. FELLOUS, A. M. LENNON, and J. NUNEZ. 1977. Is Thyroxine a regulatory signal for neurotubule assembly during brain development? *Nature (Lond.).* **266**:188–190.
15. FUGE, H. 1974. Ultrastructure and function of the spindle apparatus microtubules and chromosomes during nuclear division. *Protoplasma.* **82**:289–320.
16. GASKIN, F., C. R. CANTOR, and M. L. SHELANSKI. 1974. Turbidometric studies of the *in vitro* assembly and disassembly of porcine neurotubules. *J. Mol. Biol.* **89**:737–758.
17. GOODMAN, D. B. P., H. RASMUSSEN, F. DIBELLA, and C. E. GUTHROW, JR. 1970. Cyclic adenosine 3′:5′-monophosphate-stimulated phosphorylation of isolated neurotubule subunits. *Proc. Natl. Acad. Sci. U. S. A.* **67**:652–659.
18. GOULD, R. R., and G. G. BORISY. 1977. The pericentriolar material in Chinese hamster ovary cells nucleates in microtubule formation. *J. Cell Biol.* **73**:601–615.
19. GOULD, R. R., and G. G. BORISY. 1978. Quantitative initiation of microtubule assembly by chromosomes from Chinese hamster ovary cells. *Exp. Cell Res.* **113**:369–374.
20. GRIMSTONE, A.V., and A. KLUG. 1966. Observations on the substructure of flagellar fibers. *J. Cell Sci.* **1**:351–363.
21. HYAMS, J., and G. G. BORISY. 1978. Nucleation of microtubules in vitro by isolated spindle pole bodies of the yeast *Saccharomyces cerevisiae*. *J. Cell Biol.* **78**:401–414.
22. JOHNSON, K. A., and BORISY, G. G. 1977. Kinetics of microtubule self assembly. *J. Mol. Biol.* **117**:1–31.
23. KIRSCHNER, M. W., L. S. HONIG, and R. C. WILLIAMS. 1975. Quantitative electron microscopy of microtubule assembly *in vitro*. *J. Mol. Biol.* **99**:263–276.
24. KURIYAMA, R. 1975. Further studies of tubulin polymerization *in vitro*. *J. Biochem.* **77**:23–31.
25. KURIYAMA, R., and T. MIKI-NOUMURA. Light-microscopic observations of individual microtubules reconstituted from brain tubulin. *J. Cell Sci.* **19**:607–620.
26. LOVELAND, R. P. 1933. Production of a darkfield motion photo micrograph which exhibit flagella in motile bacteria. *J. Biol. Photogr. Assoc.* **1**:128–135.
27. LOWRY, O. H., N. J. ROSEBROUGH, A. L. FARR, and R. J. RANDALL. 1951. Protein measurement with the folin reagent. *J. Biol. Chem.* **193**: 265–275.
28. MCGILL, M., and B. R. BRINKLEY. 1975. Human chromosomes and centrioles as nucleation sites for the in vitro assembly of microtubules from bovine brain tubulin. *J. Cell Biol.* **67**:189–199.
29. MARGOLIS, R. L., and L. WILSON. 1978. Opposite end assembly and disassembly of microtubules at steady state *in vitro*. *Cell.* **13**:1–8.
30. MURPHY, D. B., and G. G. BORISY. 1975. Association of high molecular weight proteins with microtubules and their role in microtubule assembly *in vitro*. *Proc. Natl. Acad. Sci. U. S. A.* **72**:2696–2700.
31. OLMSTED, J. B., MARCUM, J. M., JOHNSON, K. A., ALLEN, C., and G. G. BORISY. 1974. Microtubule assembly: some possible regulatory mechanisms. *J. Supramol. Struct.* **2**:529–450.
32. PICKETT-HEAPS, J. D. 1969. The evolution of the mitotic apparatus: an attempt at comparative ultrastructural cytology in dividing plant cells. *Cytobios.* **1**(3):257–380.
33. RAYBIN, D., and M. FLAVIN. 1977. An enzyme which specifically adds tyrosine to alpha chain of tubulin. *Biochemistry* **16**:2189–2194.
34. ROBBINS, E., and N. K. GONATAS. 1964. The ultrastructure of a mammalian cell during the mitotic cycle. *J. Cell Biol.* **21**:429–463.
35. ROOS, V.-P. 1973. Light and electron microscopy of rat kangaroo cells in mitosis. I. Formation and breakdown of the mitotic apparatus. *Chromosoma (Berl.).* **40**:43–82.
36. SALMON, E. P., D. GOOD, T. K. MAUGEL, and D. B. BONAR. 1976. Pressure-induced depolymerization of spindle microtubules. III. Differential stability in HeLa cells. *J. Cell Biol.* **69**:443–454.
37. SANDOVAL, I. V., and P. CUATRECASAS. 1976. Protein kinase associated with tubulin affinity chromatography and properties. *Biochemistry.* **15**: 3429–3432.
38. SCHEELE, R. B., T. M. SCHUSTER, and L. H. KHAIRALLAH. 1973. TMV protein: a metastable polymerization state. *Biophys. Soc. Annu. Meet.*

Abstr. **17**:290*a*.

39. SCHMITT, H., R. JOSEPHS, and E. REISLER. 1977. A search for *in vivo* factors in regulation of tubulin assembly. *Nature (Lond.).* **265**:653–655.
40. SLOBODA, R. D., S. A. RUDOLPH, J. L. ROSENBAUM, and P. GREENGARD. 1975. Cyclic AMP-dependent endogenous phosphorylation of a microtubule associated protein. *Proc. Natl. Acad. Sci. U. S. A.* **72**:177–181.
41. SLOBODA, R. D., W. L. DENTLER, R. A. BLOODGOOD, B. R. TELZER, S. GRANETT, and J. L. Rosenbaum. 1976. Microtubule associated proteins (MAPs) and the assembly of microtubules *in vitro*. *In* Cell Motility. Book C. R. Goldman, T. Pollard, and J. Rosenbaum, editors. Cold Spring Harbor Laboratory, Cold Spring Harbor, N. Y. 1171–1212.
42. SLOBODA, R. D., W. L. DENTLER, and J. L. ROSENBAUM. 1976. Microtubule associated proteins and stimulation of tubulin assembly *in vitro*. *Biochemistry.* **15**:4497–4505.
43. SNELL, W. J., W. L. DENTLER, L. T. HAIMO, L. I. BINDER, and J. L. ROSENBAUM. 1974. Assembly of chick brain tubulin onto isolated basal bodies of *Chlamydomonas reinhardtii*. *Science (Wash. D. C.).* **185**:357–359.
44. SNYDER, J. A., and J. R. MCINTOSH. 1975. Initiation growth of microtubules from mitotic centers in lysed mammalian cells. *J. Cell Biol.* **67**: 744–760.
45. STEARNS, M. E., J. A. CONNOLLY, and D. L. BROWN. 1976. Cytoplasmic microtubule organizing centers isolated from *Polytomella agelis*. *Science (Wash. D. C.).* **191**:188–191.
46. SUMMERS, K. E., and I. R. GIBBONS. 1971. Adenosine triphosphate-induced sliding of tubules in tyrosine-treated flagella of sea urchin sperm. *Proc. Natl. Acad. Sci. U. S. A.* **68**:3092–3096.
47. SUMMERS, K., D. RAYBIN, and M. FLAVIN. 1975. Complex mechanism of microtubule polymerization observed in darkfield light microscopy. *J. Cell Biol.* **67**(2. Pt. 2):422*a*. (Abstr.).
48. TELZER, B. R., M. J. MOSES, and J. L. ROSENBAUM. 1975. Assembly of microtubules onto kinetochores of isolated mitotic chromosomes of HeLa cells. *Proc. Natl. Acad. Sci. U. S. A.* **72**:4023–4027.
49. TOYOHARA, A., SHIGENAKA, Y., and H. MOHRI. 1978. Microtubules in protozoan Cells. III. Ultrastructural changes during disintegration and reformation of heliozoan microtubules. *J. Cell Sci.* **32**:87–98.
50. TUCKER, J. B. 1971. Spatial discrimination in the cytoplasm during microtubule morphogenesis. *Nature (Lond.).* **232**:387–390.
51. WEINGARTEN, M. D., M. M. SUTER, D. R. LITTMAN, and M. W. KIRSCHNER. 1974. Properties of the depolymerization products of microtubules from mammalian brain. *Biochemistry* **13**:5529–5537.
52. WEINGARTEN, M. D., A. H. LOCKWOOD, S.-Y. HWO, and M. W. KIRSCHNER. 1975. A protein factor essential for microtubule assembly. *Proc. Natl. Acad. Sci. U. S. A.* **72**:1858–1862.
53. WEISENBERG, R. C., G. G. BORISY, and E. W. TAYLOR. 1968. The colchicine binding protein of mammalian brain and its relation to microtubules. *Biochemistry.* **7**:4466–4479.
54. WITMAN, G. B., D. W. CLEVELAND, M. D. WEINGARTEN, and M. W. KIRSCHNER. 1976. Tubulin requires tau for growth onto microtubule initiation sites. *Proc. Natl. Acad. Sci. U. S. A.* **73**:4070–4074.